PERGAMON

International Journal of Heat and Mass Transfer 45 (2002) 1525–1534

International Journal of HEAT and MASS TRANSFER

www.elsevier.com/locate/ijhmt

A linear and non-linear analysis on interfacial instability of gas–liquid two-phase flow through a circular pipe

Lie-Jin Guo *, Guang-Jun Li, Xue-Jun Chen

State Key Laboratory of Multiphase Flow in Power Engineering, Xi'an Jiaotong University, Xi'an, Shaanxi Province 710049, China

Received 6 November 2000; received in revised form 12 June 2001

Abstract

A linear instability analysis was conducted firstly on the interface of a stratified gas–liquid two-phase flow in a circular piper employing a two-fluid model. The constitutive equations simulation technique was discussed, and the dispersive equation of interfacial waves was derived. The effects of flow rates of gas and liquid, liquid viscosity, surface tension and tube inclination on the stability of interface were investigated. A set of non-linear hyperbolic governing equations was deduced from the complete two-fluid model equation by omitting the effect of the surface tension and assuming a quasi-steady-state for the gas phase. Using characteristic line and finite difference, the propagation and growth of the interfacial disturbances were investigated in terms of gas and liquid superficial velocities. Then the results of the non-linear stability analysis were compared with those obtained by the linear stability analysis and experimental data. The non-linear stability analysis not only confirms the conclusions reached by the linear instability analysis, but also gives an insight into the growth and propagation of the interfacial disturbances on the interface of a gas–liquid two-phase flow.

Keywords: Gas–liquid two-phase flow; Interfacial waves; Linear and non-linear stability analysis; Characteristic line; Numerical simulation

1. Introduction

Interfacial waves which exist on the interface of a gas–liquid two-phase flow have a significant effect on the heat and mass transfer of a two-phase flow, and also on the pressure drop characteristics of the system. Obviously it is of importance to understand these phenomena. As early as in 1950s, Banjamin [1], Miles [2], Hanratty and Hershman [3], Hanratty and Engen [4] noted and studied this kind of problem. One of the main problems is the stability analysis of two-phase interface. In the previous study, most of the researchers used integrated liquid momentum equations, as Hanratty and Engen [4] and Jeffreys [5]. The effects of the gas phase on the stability were considered as the boundary conditions of the liquid momentum equations. Other researchers [6] used the Navier–Stokes equations simplified according to the problems. Recently, Brauner and Maron [7], Barnea and Taitel [8] investigated interface stability by using a two-fluid two-phase flow model.

In the present work, using a two-fluid model the stability analysis was conducted for a gas–liquid two-phase flow, and the constitutive equations were specially discussed. The dispersive equation of interfacial waves was derived, and the effects of flow and geometrical conditions (such as tube inclination β) on the stability were investigated.

A set of non-linear hyperbolic governing equations was also deduced from the complete two-fluid model equation by omitting the effect of the surface tension and assuming a quasi-steady-state for the gas phase. The propagation and growth of the interfacial disturbances were investigated by using the numerical method in terms of gas and liquid superficial velocities. The non-linear stability analysis further confirmed the conclusions reached by the linear instability analysis, and provided a comprehensive understanding of the physical

* Corresponding author. Tel.: +86-29-266-3895; fax: +86-29-266-9033.

E-mail address: lj-guo@xjtu.edu.cn (L.-J. Guo).

0017-9310/02/$ - see front matter
PII: S0017-9310(01)00247-2

Nomenclature

A	cross-section, m^2
A_k	the area occupied by phase $k = 1, g$
C	friction factor, dimensionless
c	wave velocity, m/s
D	tube diameter, m
f	see Eq. (7), N/m^3
g	gravity acceleration, m/s^2
h	liquid film thickness, m
$\overline{h}$	steady-state solution to liquid film thickness, m
h'	small disturbance of h, m
$\dot{h}$	wave amplitude, m
K	wave number, l/mp
p	area averaged pressure, Pa
p_{ik}	pressure on the interface, Pa
S	wetted perimeter, m
S_i	interface width, m
t	time, s
u	area averaged velocity, m/s
u_k''	instantaneous velocity of phase k,
u'	small disturbance of u, m/s
$\overline{u}$	steady-state solution for velocity, m/s
$\dot{u}$	wave amplitude, m/s
x	flow direction, m
y	vertical to flow direction, m
β	tube inclination, positive for down flow, °
Γ	velocity shape factor, dimensionless
λ	wavelength, m
λ^*	non-dimensional wavelength (λ/D)
μ	dynamic viscosity, Pa s
ν	kinematic viscosity, m^2/s
ρ	density, kg/m^3
σ	surface tension, N/m
τ	shear stress, Pa
τ_ℓ	interfacial shear stress, Pa
Kc_ℓ	ordinate amplification factor

Subscript

g	gas phase
I, R	imaginary, real part
ℓ	liquid phase
s	superficial
k	phase k, $k = 1, g$
i	interface

nature, specifically an insight into the growth and propagation of the interfacial disturbances on the interface of a gas–liquid two-phase flow.

2. Two-fluid model

Fig. 1 illustrates the configuration of a gas–liquid two-phase stratified flow. Some assumptions were introduced as

- no heat transfer between two phase;
- no mass transfer between two phase;
- both gas and liquid incompressible.

The one-dimensional integrated equations of two fluid models are as follows:

$$\frac{\partial}{\partial t}(\rho_k A_k) + \frac{\partial}{\partial x}(\rho_k A_k u_k) = 0, \tag{1}$$

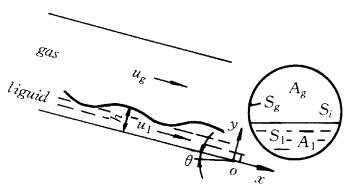

Fig. 1. Configuration of gas–liquid two-phase stratified flow.

$$\frac{\partial}{\partial t}(\rho_k A_k u_k) + \frac{\partial}{\partial x}(\rho_k \Gamma_k u_k^2) = -\tau_k S_k \pm \tau_i S_i + \rho_k g A_k \sin\beta - \frac{\partial}{\partial x}(A_k p_k) + p_{ik}\frac{\partial A_k}{\partial x}. \tag{2}$$

Upper sign of "±" corresponds to the liquid phase. Γ_k is the velocity shape factor of phase k, and it is defined by

$$\Gamma_k = \frac{1}{A_k u_k^2}\int\int_{A_k} u_k''^2 \, dA_k, \tag{3}$$

$\Gamma_k = 1$ [9] for plug flow, $\Gamma_t = 4/3$ [10] for a very thin turbulent shear layer, $\Gamma_t = 1.6$ for thin turbulent shear layer. In this work $\Gamma_k = 1$. For simplification we assume that the interfacial waves have a large wavelength compared with the liquid film thickness. Therefore the shallow water and shallow gas conditions can be met, that means the pressure in phase k is only affected by the hydrostatic head rather than the interfacial conditions. So the pressure in phase k can be defined by

$$p_k' = p_{ik} - \rho_k g \cos\beta (y - h), \tag{4}$$

$p_{ig} \neq p_{i\ell}$, if the surface tension, σ, is considered, and the difference is expressed as

$$\frac{\partial}{\partial x}(p_{ig} - p_{i\ell}) = -\frac{\partial}{\partial x}\left\{\frac{\partial^2 h}{\partial x^2}\Big/\left[1 + \left(\frac{\partial h}{\partial x}\right)^2\right]^{2/3}\right\}. \tag{5}$$

From Eqs. (1), (2), (4) and (5) the combined two-phase momentum equation is deduced:

$$\left[\rho_\ell(1-\Gamma_\ell)\frac{u_\ell}{A_\ell}+\rho_{\rm g}(1-\Gamma_{\rm g})\frac{u_{\rm g}}{A_{\rm g}}\right]\frac{{\rm d}A_\ell}{{\rm d}h}\frac{\partial h}{\partial t} + (\rho_\ell-\rho_{\rm g})g\cos\beta\frac{\partial h}{\partial x}+\frac{\partial}{\partial x}(p_{{\rm i}\ell}-p_{{\rm i}{\rm g}}) + \rho_\ell\frac{\partial u_\ell}{\partial t}+\rho_\ell\Gamma_\ell u_\ell\frac{\partial u_\ell}{\partial x}-\rho_{\rm g}\frac{\partial u_{\rm g}}{\partial t}-\rho_{\rm g}\Gamma_{\rm g}u_{\rm g}\frac{\partial u_{\rm g}}{\partial x}=f, \tag{6}$$

where

$$f=-\tau_\ell S_\ell/A_\ell+\tau_{\rm i}S_{\rm i}(1/A_\ell+1/A_{\rm g})+(\rho_\ell-\rho_{\rm g})g\sin\beta. \tag{7}$$

3. Linear stability analysis

3.1. Dispersive equation of the interfacial waves

Introducing the following parameters:

$$\begin{aligned} h&=\overline{h}+h',\\ u_\ell&=\overline{u}_\ell'+u_\ell',\\ u_{\rm g}&=\overline{u}_{\rm g}+u_{\rm g}', \end{aligned} \tag{8}$$

where $\overline{h}$, $\overline{u}_\ell$, $\overline{u}_{\rm g}$ were obtained by solving the fully developed stratified flow for a set of flow rates of the two-phase flow, and h', u_ℓ', $u_{\rm g}'$ are the small disturbance values of h, u_ℓ, $u_{\rm g}$, respectively. A small amplitude disturbance is imposed on the interface as follows:

$$h'=h{\rm e}^{{\rm i}K(x-ct)}. \tag{9}$$

When $c_1>0$, the small disturbances grow; $c_1<0$, they decay. Let $c_1=0$, and neutral stability condition is obtained. The maximum Kc_ℓ corresponds to the amplification factor of the fastest growing waves.

For a small value of h', the change of the film thickness induces a linear response of u_ℓ, $u_{\rm g}$, or

$$\frac{h'}{h}=\frac{u_\ell'}{\hat{u}_\ell}=\frac{u_{\rm g}'}{\hat{u}_{\rm g}}={\rm e}^{{\rm i}K(x-ct)}. \tag{10}$$

Substituting Eq. (10) into Eqs. (1) and (6) and omitting the higher order of the small disturbance, we get the dispersive equation of the interfacial waves as follows (for the details, refer to [7], or [8]):

$$a_1c^2-2(a_2+{\rm i}a_3)c+a_4+{\rm i}a_5=0, \tag{11}$$

where

$$a_1=\rho_\ell A_\ell'/A_\ell+\rho_{\rm g}A_\ell'/A_{\rm g},$$

$$a_2=\rho_\ell A_\ell'/A_\ell[1+(\Gamma_\ell-1)/2]\overline{u}_\ell+\rho_{\rm g}(A_\ell'/A_{\rm g})\times[1+(\Gamma_\ell-1)/2]\overline{u}_{\rm g},$$

$$a_3=\frac{1}{2K}\left(\frac{A_i'\partial F}{A_\ell\partial u_\ell}-\frac{A_\ell'\partial F}{A_{\rm g}\partial u_{\rm g}}\right),$$

$$a_4=\rho_\ell\frac{A_\ell'}{A_\ell}\Gamma_\ell\overline{u}_\ell^2+\rho_{\rm g}\frac{A_\ell'}{A_\ell}\Gamma_{\rm g}\overline{u}_{\rm g}^2-[(\rho_\ell-\rho_{\rm g})g\cos\beta+\sigma k^2],$$

$$a_5=\frac{1}{K}\left(\frac{A_\ell'}{A_\ell}\overline{u}_\ell\frac{\partial F}{\partial\overline{u}_\ell}-\frac{A_\ell'}{A_{\rm g}}\overline{u}_{\rm g}\frac{\partial F}{\partial\overline{u}_{\rm g}}-\frac{\partial F}{\partial\Gamma_\ell}\right).$$

The solutions of Eq. (11) are

$$c_{1,2}=\frac{a_2+{\rm i}a_3\pm\sqrt{(a_2+{\rm i}a_3)^2-a_1(a_4+{\rm i}a_5)}}{a_1}, \tag{12}$$

a_3, and a_4 come from the shear stress terms in Eq. (6). For inviscid flow, $a_3=a_5=0$. From Eq. (12) the inertia terms in a_4 are instability factors, but gravity and surface tension terms are stability factors.

3.2. Constitutive equations

The fully developed stratified gas–liquid two-phase flow was solved to obtain $\overline{h}$, $\overline{u}_\ell$, $\overline{u}_{\rm g}$ by using Taitel and Dukler's method, and the geometrical parameters, such as A_ℓ, $A_{\rm g}$, S, etc., were obtained simultaneously. Taital and Dukler [11], Brauner and Maron [7] gave some formulas for calculating these geometrical parameters. The shear stress τ is a key parameter to solve the equation. Here we used the pseudo-steady assumption, that means the shear stress only related to the fully developed solution

$$\begin{aligned} \tau_{\rm g}&=f_{\rm g}\rho_{\rm g}\frac{\overline{u}_{\rm g}^2}{2},\\ \tau_\ell&=\rho_\ell f_\ell\frac{\overline{u}_\ell^2}{2},\\ \tau_{\rm g}&=f_{\rm g}\frac{\rho_{\rm g}(\overline{u}_{\rm g}-\overline{u}_\ell)^2}{2}, \end{aligned} \tag{13}$$

$f_{\rm g}$, f_ℓ were defined, respectively, by the following Blasius equation:

$$\begin{aligned} &f_{\rm g}=c_{\rm g}\left(\frac{D_{\rm g}\overline{u}_{\rm g}}{v_{\rm g}}\right)^{-n_{\rm g}},\quad f_\ell=c_\ell\left(\frac{D_\ell\overline{u}_\ell}{v_\ell}\right)^{-n_\ell},\\ &D_\ell=4A_\ell/S_\ell,\quad D_{\rm g}=\frac{4A_{\rm g}}{S_{\rm g}+S_\ell}, \end{aligned} \tag{14}$$

$c_{\rm g}=c_\ell=16$, $n_{\rm g}=n_\ell=1$ for laminar flow; $c_{\rm g}=c_\ell=0.046$, $n_{\rm g}=n_\ell=0.2$ for turbulent flow. f_ℓ was given by Kowalski [12] as follows:

$$f_\ell=2\left[0.804(Re_{\rm g}^*)^{-0.285}\right]^2, \tag{15}$$

where

$$Re_{\rm g}^*=\frac{D_{\rm g}\overline{u}_{\rm g}}{v_{\rm g}}.$$

3.3. Calculating procedure

Eq. (11) is a quadratic equation with complex coefficients. It is very easy to find the solutions to it. The calculated sequence is given as follows:

- Input the known parameters including gas and liquid flow rates and geometrical parameter.
- Solving the fully developed stratified gas–liquid flow for $\overline{h}$, $\overline{u}_g$, $\overline{u}_\ell$.
- Calculating the coefficients of Eq. (11).
- Solving Eq. (11) to obtain the results.

It is noted that in the calculation, air was used as gas phase, water as liquid phase, and the pressure of flow system is atmospheric pressure.

3.4. Results

Fig. 2 shows the effects of superficial velocity of liquid on the amplification factor. From Fig. 2(a), it is seen that there is a maximum value for each curve. This value stands for the amplification factor of the fastest growing waves, $(Kc_\ell)_{max}$. The wavelength of the fastest growing waves is represented by λ_{max}. $(Kc_\ell)_{max}$ decreases very rapidly as the liquid superficial velocity decreases. The points at which Kc_ℓ becomes zero are defined as the neutral stability points, P_N, the corresponding wavelength of the waves is defined as the neutral wave wavelength, λ_N, tending to be smaller when the liquid superficial velocity $U_{\ell s}$ increases. An enlarged picture is shown in Fig. 2(b) to show the behavior at a low amplification factor. In this figure, the details in the vicinity of neutral stability can be observed. When $U_{\ell s}$ equals 0.1 or 0.05 m/s, $Kc_\ell < 0$ for the whole range of wavelengths, and it means that any disturbance on the two-phase interface will decay with time in this case and the flow is stable.

Fig. 3 shows the effects of the gas superficial velocity U_{gs}. The effect is very similar to that of $U_{\ell s}$. With increasing the U_{gs}, $(Kc_\ell)_{max}$ increases, while λ_N decreases and the neutral point moves to the left.

The effect of tube inclination β (positive for down flow) on the amplification factor is shown in Fig. 4. Apparently upward flow is less stable than downward flow, and tube inclination has an effect on the neutral stability point P_N and the fastest growing wave wavelength λ_{max}. With increasing tube inclination β (from downward flow to upward flow), λ_{max} decreases and P_N moves to the left.

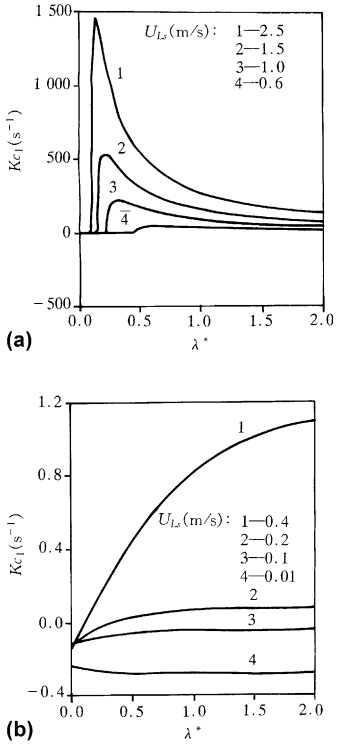

Fig. 2. Effect of $U_{\ell s}$ on the amplification factor ($U_{gs} = 5$ m/s, $\beta = 0°$, $\mu = 7.97 \times 10^{-4}$ Pa s, $\sigma = 0.072$ N/m).

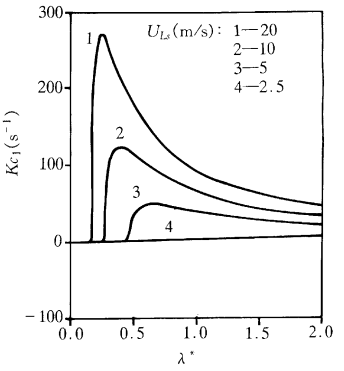

Fig. 3. Effect of U_{gs} on the amplification factor ($U_{\ell s} = 0.6$ m/s, $\beta = 0°$, $\mu = 7.97 \times 10^{-4}$ Pa s, $\sigma = 0.072$ N/m).

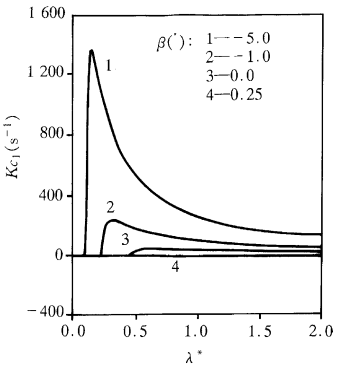

Fig. 4. Effect of β on the amplification factor ($U_{gs} = 5$ m/s, $U_{\ell s} = 0.6$ m/s, $\mu = 7.97 \times 10^{-4}$ Pa s, $\sigma = 0.072$ N/m).

Liquid viscosity has different effects on the amplification factor Kc_ℓ from those of other parameters, as seen in Fig. 5. With increasing liquid viscosity, Kc_ℓ increases, λ_{max} decreases, and the neutral stability point P_N moves to the left. But when liquid viscosity equals 3×10^{-2} Pa s, the amplification factor Kc_ℓ decreases, curve 4 in Fig. 5, its characteristics are just the same as those of curve 2 with liquid viscosity 7.97×10^{-4} Pa s. Further calculated results are shown in Fig. 8.

Fig. 6 shows the effects of surface tension on the amplification factor, greatly altering the values of Kc_ℓ especially the wavelength of the fastest growing waves and the neutral stability point. With increasing surface tension, Kc_ℓ decreases, λ_{max} increases and the neutral stability point moves to the right. But the surface tension has a great influence on Kc_ℓ only within a short wavelength regime. When the wavelength reaches a certain large value, there are no explicit differences between curves 1, 2, and 3.

The effects of gas and liquid superficial velocity on the characteristics of interfacial waves are given in Fig. 7. Within the range in which we are interested, with increasing U_{gs} and $U_{\ell s}$, Kc_ℓ increases and λ_{max}, λ_N decrease

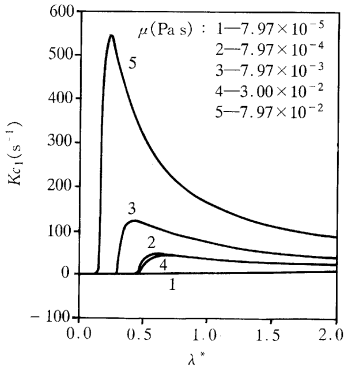

Fig. 5. Effect of liquid viscosity on the amplification factor ($U_{gs} = 5$ m/s, $U_{\ell s} = 0.6$ m/s, $\beta = 0°$, $\sigma = 0.072$ N/m).

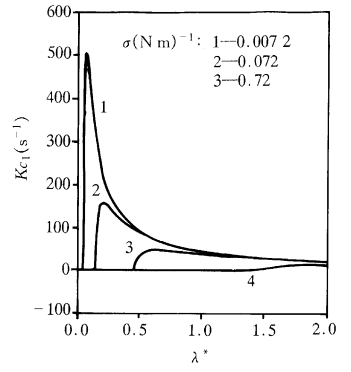

Fig. 6. Effect of surface tension on the amplification factor ($U_{gs} = 5$ m/s, $U_{\ell s} = 0.6$ m/s, $\beta = 0°$, $\mu = 7.97 \times 10^{-4}$ Pa s).

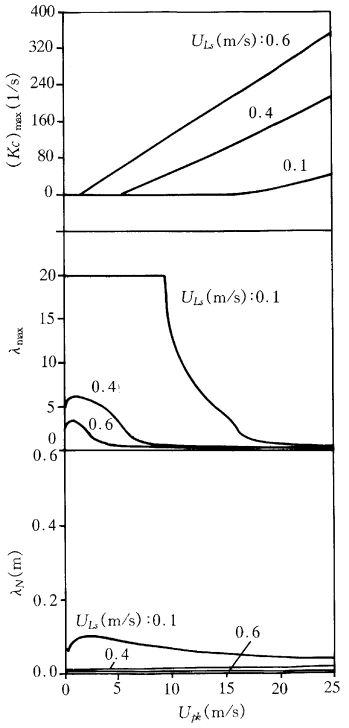

Fig. 7. Effect of U_{gs} on $(Kc_\ell)_{max}$, λ_{max}, λ_N ($\beta = 0°$, $\mu = 7.97 \times 10^{-4}$ Pa s, $\sigma = 0.072$ N/m).

as the increase of U_{gs} and $U_{\ell s}$. The λ_{max} remains 20 when $U_{\ell s}$ equals 0.1 m/s and U_{gs} is less than 9 m/s, which means under this condition there are no notable maximum points in the amplification curve, such as curves 2, 3, and 4 in Fig. 2(b).

Fig. 8 shows the effects of liquid viscosity on the above parameters. The influences of liquid viscosity on $(Kc_\ell)_{max}$, λ_{max}, λ_N are very complex. When the liquid viscosity is in a certain regime, referring to Fig. 8, $(Kc_\ell)_{max}$ decreases, λ_{max} and λ_N increase, but beyond this regime, $(Kc_\ell)_{max}$ increases, λ_{max} and λ_N decrease. The effects of liquid viscosity on the amplification factor of interfacial waves are very puzzling. It is generally known that the higher the liquid viscosity is, the more stable the flow is. According to the traditional theory, any flow will be stable when the liquid viscosity is high enough. However, with increasing liquid viscosity, we found that the liquid holdup increased firstly, and at a certain liquid viscosity, it decreased suddenly, and then increased. Up to now, we did not find a reasonable explanation for these results. This needs further investigations.

4. Non-linear interfacial stabilities analysis

As known from the above section, the linear stability analysis can be only used to distinguish that an interface

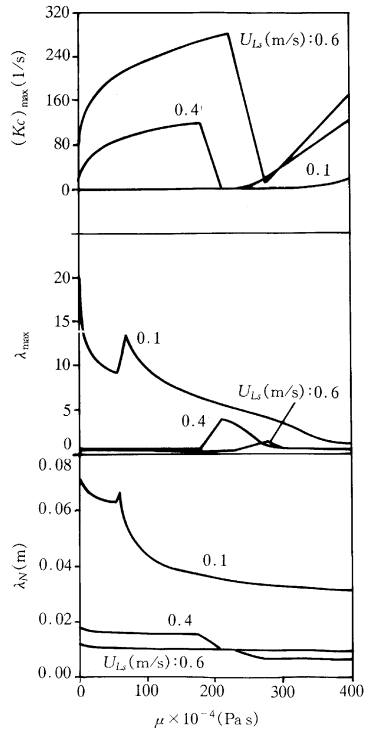

Fig. 8. Effect of μ on $(Kc_\ell)_{\max}$, $\lambda_{\max}$, λ_N ($U_{gs} = 10$ m/s, $\beta = 0°$, $\sigma = 0.0723$ N/m).

is stable or not, but not to obtain the details of development of the disturbance on the interfacial surface. The characteristics of the formation and growing up of the disturbances or dynamic process on the interface have to be analyzed by non-linear methods. In the following sections, we have attempted to do this from the complete two-fluid model.

4.1. Non-linear equation and their characteristic equations

For a gas–liquid two-phase inclined stratified flow, as shown in Fig. 1, the following assumptions were introduced:

- no heat and mass transfer between two phase;
- no phase change occurs;
- both gas and liquid are incompressible, and the gas phase can be considered at quasi-steady-state condition.

The set of non-linear equations was be deduced by omitting the pressure terms in the momentum equation from the one-dimensional equations of a two-fluid model as follows:

$$\frac{\partial h}{\partial t} + u_\ell \frac{\partial h}{\partial x} + \frac{A_\ell}{A_\ell} \frac{\partial u_\ell}{\partial x} = 0, \tag{16}$$

$$G\frac{\partial h}{\partial x} + \frac{\partial u_\ell}{\partial t} + u_\ell \frac{\partial u_\ell}{\partial x} - \frac{\sigma}{\rho_\ell} \frac{\partial^3 h}{\partial x^3} + E = 0. \tag{17}$$

Here,

$$A'_\ell = \frac{\mathrm{d}A_\ell}{\mathrm{d}h},$$

$$G = \frac{(\rho_\ell - \rho_g) d \cos\theta}{\rho_\ell} - \frac{\rho_g A^2 j_g^2 A'_\ell}{\rho_\ell A_g^3},$$

$$E = -\frac{\Delta f}{\rho_\ell},$$

$$\Delta f = -\frac{\tau_\ell S_\ell}{A_\ell} + \frac{\tau_g S_g}{A_g} + \tau_i S_i \left(\frac{1}{A_\ell} + \frac{1}{A_g}\right) + (\rho_\ell - \rho_g) g \sin\theta.$$

Because the surface tension σ has less influence on the neutral instability condition and the interfacial waves have a large wavelength compared to the liquid film thickness in the range of parameters studied, and the effects of the surface tension σ can be neglected [13]. So Eqs. (16) and (17) become a set of standard non-linear hyperbolic governing equations and can be rewritten as

$$\frac{\partial Y}{\partial t} + Z\frac{\partial Y}{\partial x} + F = 0, \tag{18}$$

where

$$Y = [h, u_\ell]^{\mathrm{T}},$$

$$F = [0, E]^{\mathrm{T}},$$

$$Z = \begin{bmatrix} u_\ell & A_\ell/A'_\ell \\ G & u_\ell \end{bmatrix}.$$

Two characteristic values of matrix $\mathbf{Z}$ are as follows:

$$\begin{aligned} \lambda_1 &= u_\ell + (GA_\ell/A'_\ell)^{1/2}, \\ \lambda_2 &= u_\ell - (GA_\ell/A'_\ell)^{1/2}, \end{aligned} \tag{19}$$

λ_1, λ_2 are, respectively, corresponding to the two propagation velocities of disturbances in physics. When $\lambda_2 > 0$, the flow is supercritical flow; when $\lambda_2 < 0$, the flow is sub-critical flow.

Assume $D = |D_{ij}|$ is the matrix for characteristic vector of matrix $\mathbf{Z}$ [14,15], that is,

$$\mathbf{DZ} = \Lambda\mathbf{D}, \tag{20}$$

where

$$\Lambda = \begin{bmatrix} \lambda_\ell & 0 \\ 0 & \lambda_2 \end{bmatrix},$$

$$D = \begin{bmatrix} 1/B & 1 \\ 1/B & -1 \end{bmatrix},$$

$$B = \left(\frac{A_\ell}{A'_\ell G}\right)^{1/2}.$$

By multiplying Eq. (18) by the matrix for characteristic vector $\mathbf{D}$ on the left-hand side, a set of characteristics equations was deduced and the form of fractions as follows:

For the first characteristic value $dx/dt = \lambda_1$,

$$\frac{\partial h}{\partial t} + \lambda_1 \frac{\partial h}{\partial x} + B\left(\frac{\partial u_\ell}{\partial t} + \lambda_1 \frac{\partial u_\ell}{\partial x}\right) + BE = 0. \tag{21}$$

For the first characteristic value $dx/dt = \lambda_2$,

$$\frac{\partial h}{\partial t} + \lambda_2 \frac{\partial h}{\partial x} + B\left(\frac{\partial u_\ell}{\partial t} + \lambda_2 \frac{\partial u_\ell}{\partial x}\right) + BE = 0. \tag{22}$$

4.2. Difference scheme for characteristics equations

Because the characteristics equations derived are strong non-linear ones, the two characteristic values of the equations are variable to be solved, and it is very difficult to construct the difference scheme by the typical characteristics method. An improved and simplified characteristics line method was employed to discretize the characteristics equation (21) or (22) [14].

By using difference scheme for time variable, that is,

$$\begin{aligned} \frac{\partial h}{\partial t} &= \frac{h_i^{n+1} - h_i^n}{\Delta t}, \\ \frac{\partial u_\ell}{\partial t} &= \frac{(u_\ell)_i^{n+1} - (u_\ell)_i^n}{\Delta t}. \end{aligned} \tag{23}$$

By using upwind difference scheme for space variables, that is,

$$\begin{aligned} \lambda_i \frac{\partial h}{\partial x} &= \begin{cases} \frac{\lambda_i}{\Delta x}(h_i^n - h_{i-1}^n), & \lambda_i \geqslant 0, \\ \frac{\lambda_i}{\Delta x}(h_{i+1}^n - h_i^n), & \lambda_i < 0, \end{cases} \\ \lambda_i \frac{\partial u_\ell}{\partial x} &= \begin{cases} \frac{\lambda_i}{\Delta x}[(u_\ell)_i^n - (u_\ell)_{i-1}^n), & \lambda_i \geqslant 0, \\ \frac{\lambda_i}{\Delta x}[(u_\ell)_{i+1}^n - (u_\ell)_i^n), & \lambda_i < 0. \end{cases} \end{aligned} \tag{24}$$

Eqs. (21), (22) can be discretized by using Eqs. (23), (24) and be combined to seek for their solutions, then the values of h, u_ℓ at next time step can be obtained as follows:

When $\lambda_2 \geqslant 0$

$$\begin{aligned} h_i^{n+1} = h_i^n &- \frac{(\lambda_1)_i + (\lambda_2)_i}{2}\frac{\Delta t}{\Delta x}\left(h_i^n - h_{i-1}^n\right) \\ &- \frac{B_i[(\lambda_1)_i + (\lambda_2)_i]}{2}\frac{\Delta t}{\Delta x}\left[(u_\ell)_i^n - (u_\ell)_{i-1}^n\right], \end{aligned} \tag{25}$$

$$\begin{aligned} (u_\ell)_i^{n+1} = (u_\ell)_i^n &- \frac{(\lambda_1)_i + (\lambda_2)_i}{2B_i}\frac{\Delta t}{\Delta x}\left(h_i^n - h_{i-1}^n\right) \\ &- \frac{(\lambda_1)_i + (\lambda_2)_i}{2}\frac{\Delta t}{\Delta x}\left[(u_\ell)_i^n - (u_\ell)_{i-1}^n\right] - \Delta t E_i. \end{aligned} \tag{26}$$

When $\lambda_2 < 0$

$$\begin{aligned} h_i^{n+1} = h_i^n &- \frac{\Delta t}{2\Delta x}\left[(\lambda_2)_i h_{i+1}^n + [(\lambda_1)_i - (\lambda_2)_i]h_i^n - (\lambda_1)_i h_{i-1}^n\right] \\ &- \frac{B_i \Delta t}{2\Delta x}\left[-(\lambda_2)_i (u_\ell)_{i+1}^n + [(\lambda_1)_i + (\lambda_2)_i](u_\ell)_i^n \right. \\ &\left. - (\lambda_1)_i (u_\ell)_{i-1}^n\right], \end{aligned} \tag{27}$$

$$\begin{aligned} (u_\ell)_i^{n+1} = (u_\ell)_i^n &- \frac{\Delta t}{2B_i \Delta x}\left[-(\lambda_2)_i h_{i+1}^n + [(\lambda_1)_i \right. \\ &\left. - (\lambda_2)_i]h_i^n - (\lambda_1)_i h_{i-1}^n\right] - \frac{\Delta t}{2\Delta x}\left[(\lambda_2)_i (u_\ell)_{i+1}^n \right. \\ &\left. + [(\lambda_1)_i - (\lambda_2)_i](u_\ell)_i^n - (\lambda_1)_i (u_\ell)_{i-1}^n\right] - \Delta t E_i, \\ &i = 1, 2, 3, \ldots, N, \quad n = 0, 1, 2, \ldots, M-1. \end{aligned} \tag{28}$$

The stability criterion of the above difference scheme for space and time variables is given below [14,15]

$$\Delta t < \frac{\Delta x}{\max|\lambda_i|}.$$

4.3. Method and procedure for simulation

4.3.1. Boundary conditions

For $\lambda_2 > 0$, because all of the disturbances will spread out to backward positions, the boundary condition at $x = 0$ is the initial value at $t = 0$, the right boundary considered as an infinite, or $\Delta x \cdot N$ large enough.

For $\lambda_2 < 0$, the disturbances corresponding to the eigenvalue will spread out forwardly to upstream. At $x = 0$, because $\lambda_1 > 0$, this characteristics equation become invalid. Therefore, the boundary condition has to be added to the equation. In practice we can consider j_ℓ (the superficial liquid velocity) as a constant at $x = 0$.

4.3.2. Solving procedure

(a) set the initial conditions at $t = 0$:

$$\begin{aligned} &h(\Delta x_i, 0) = \overline{h} + h', \quad i = 0, 1, 2, \ldots, N, \\ &u_\ell(\Delta x_i, 0) = \overline{u}_\ell + u'_\ell, \quad i = 0, 1, 2, \ldots, N, \end{aligned}$$

(b) to obtain the geometric parameters and the coefficients of Eqs. (25)–(28),
(c) to solve the function values at next step of time by using the combination of Eqs. (25), (26) or (27), (28) according to the positive or negative of eigenvalue λ_2,
(d) to repeat (b) and (c) until certain time steps required are reached.

4.4. Results and discussion

4.4.1. Experimental results

By using two-parallel conductance probes, the instantaneous film thickness of a gas–liquid two-phase flow was measured experimentally in a horizontal Plexiglas pipe of 50 mm inner diameter. The characteristics including the initiation of the various interfacial wave patterns, the processes of growing up and developments of interfacial waves were investigated, and several wave patterns were distinguished through statistical analysis of signals of film thickness. The

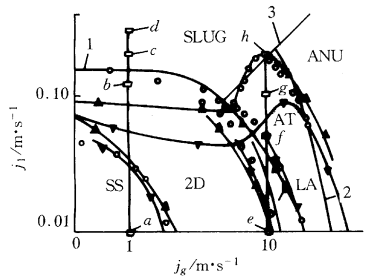

Fig. 9. The interface wave patterns and flow patterns of gas–liquid two-phase flow in a horizontal pipe. (○): results of authors; (▲): results of [6]; (▼): results of [7]. 1: Eq. (1), $c = c_{VN}$; 2: Eq. (1), $c = c_{\ell n}$; 3: $h = 0.5$.

detailed descriptions of the experiments and measurements were given in [16].

Fig. 9 shows the experimental results of wave patterns, flow patterns and their transitions obtained by authors and the comparisons with available results in [17,18], respectively obtained in a horizontal pipe of 50 mm and 25.2 mm inner diameter. In Fig. 9 SS represents the smooth stratified flow, 2D the two-dimensional waves, LA the irregular large amplitude waves, AT a new flow pattern of atomization, ANU the annular flow, and SLUG the slug flow. It was found that the transitions from each stratified wave pattern coincide approximately with those reported in previous works except for the slug flow transition boundary. Fig. 9 also illustrates the calculation results from linear stability analysis and the calculation curve 1 for $\overline{h} = 0.5$. The inception of large amplitude waves can be determined by the neutral stability criterion in the Viscous *Kelvin–Helmholtz* (VKH) analysis, shown in Fig. 9, that the disturbances on interface will decline and fall with time increase in the left side region of curve 1 where the amplification factor $Kc_I < 0$, and the disturbances on interface will be amplified with time increase in the right side region of curve 1 where the amplification factor $Kc_I > 0$. The inception of annular flow can be determined by the neutral stability criterion in the Inviscid *Kelvin-Helmholtz* (IKH) analysis, that is, the disturbances on interface will decline and fall with time increase because the amplification factor $Kc_I < 0$ in the left side region of curve 2 and the disturbances on interface will be amplified with time increase in the right side region of curve 2 where the amplification factor $Kc_I > 0$.

4.4.2. Results of non-linear analysis

Figs. 10 and 11 show the calculation results of the variation and development of the disturbances on a gas–liquid two-phase flow interfacial surface within a horizontal straight tube having an inner diameter of 50 mm, which is obtained by the non-linear analysis. The curves of $t = 0$ stand for the initial conditions for every case, where the initial disturbances were produced in the numerical simulations by adding a sine wave disturbance to the steady-state values of liquid film thickness and the disturbance amplitude was 5% of the steady-state values. In these figures all of the time intervals between two curves are 3 s, however, 0.5 s in Fig. 10(d). The time step was taken as $\Delta t = 0.1$ s and the space step $\Delta x = 0.25$ m in calculations.

Fig. 10 shows the propagation characteristics of interfacial disturbance with time increases at superficial gas velocity $j_g = 1$ m/s as the liquid velocity changes.

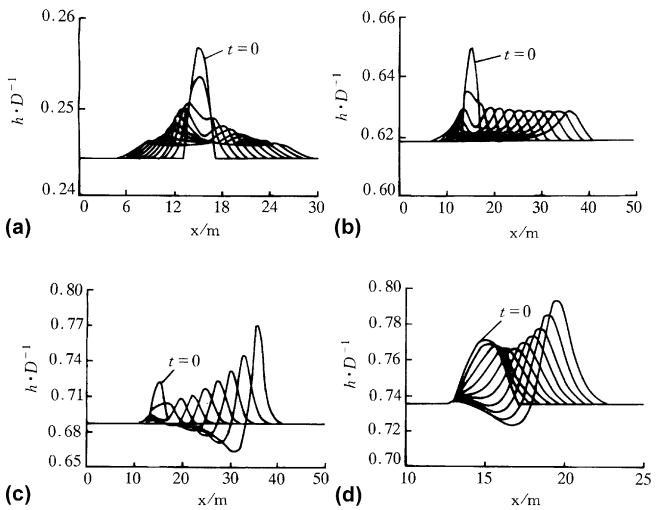

Fig. 10. The propagation and growth of interfacial disturbances in space with time under low gas velocity ($j_g = 1$ m/s). (a) $j_l = 0.01$ m/s; (b) $j_l = 0.12$ m/s; (c) $j_l = 0.2$ m/s; (d) $j_l = 0.3$ m/s.

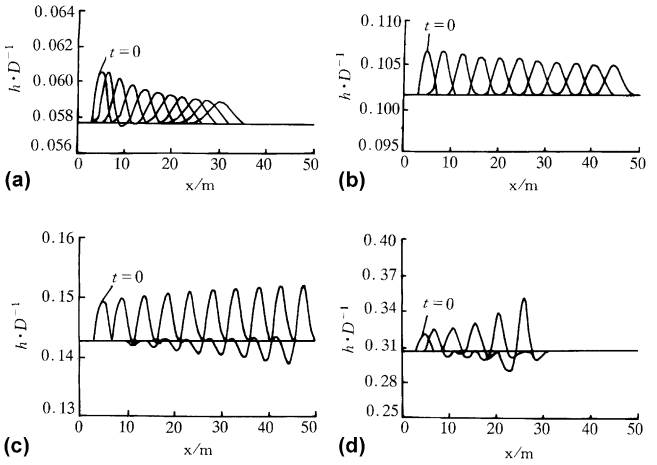

Fig. 11. The propagation and growth of interfacial disturbances in space with time under high gas velocity ($j_g = 10$ m/s). (a) $j_l = 0.01$ m/s; (b) $j_l = 0.05$ m/s; (c) $j_l = 0.1$ m/s; (d) $j_l = 0.2$ m/s.

Figs. 10(a)–(c) correspond to the sub-critical flow. The initial disturbances can be decomposed into two sets of waves in which one propagates in the upstream direction and the other propagates in the downward flow direction. The wave propagating upstream, that is, the first set of waves always becomes wider and its peak value becomes lower and declines gradually. However, the characteristics of wave propagating in the downward flow direction, that is, the second set of waves, change with the liquid velocity. Fig. 10(a) represents the case in which the second set of waves gradually declines during the propagation process. All of the disturbances existing on the interface become gradually feeble with increasing time because the amplification factor of interfacial waves $Kc_I < 0$ and the interface is smoothly stratified (SS). Fig. 10(b) illustrates the case near neutral stability wave in which the wave amplitude of the second set of waves does not change with time and correspond to the case of $Kc_I = 0$. Fig. 10(c) shows the case in which the wave amplitude of the second set of waves becomes gradually larger with increasing time up to $GA_1/A_1' < 0$ and then λ_i becomes complex and the method of characteristic lines loses effectiveness. According to the investigations in [13,19] the interfacial disturbance rapidly grew up in this case, and would block the pipe and form slug flow when $\overline{h} > 0.5$. Fig. 10(d) corresponds to the supercritical flow. The amplification factor of the second set of waves always $Kc_I > 0$, and the interface becomes more unstable with increasing time. By comparing Fig. 10 with Fig. 9, both having exactly the same operation conditions, it is found that the results of non-linear analysis coincide with the experimental data very well.

Fig. 11 shows the propagation characteristics of interfacial disturbance with time increases for high superficial gas velocity which means a very thin liquid film (generally $\overline{h} < 0.5$). Clearly, the interfacial disturbance declines gradually with time, and the influenced region of disturbance always becomes wider and its wave amplitude lower at $j_l = 0.01$ m/s. When $j_l = 0.05$ m/s, the disturbance becomes gradually weak and the interfacial wave splits during the process of propagation although the splitting phenomenon is not apparent; when $j_l = 0.1$ or 0.2 m/s, the wave splitting phenomenon is very explicit, and the disturbance becomes gradually large with time. The wave behaves like an isolated one and becomes a large amplitude wave on the gas–liquid interfacial surface [13]. Fig. 11 correspond to the four cases shown in Figs. 9(e)–(h). From the comparison of Fig. 11 with Fig. 9, the results of non-linear analysis coincide also with the experimental data very well. However, the results of linear stability analysis in this region show that the amplification factor by VKH method is $Kc_I > 0$, but the amplification factor by IKH method is $Kc_I = 0$. Very clearly, the non-linear stability analysis can give more detailed characteristic descriptions and dynamical information on the propagation behaviors of interfacial disturbance.

5. Conclusion

1. The conclusions reached from linear analysis are as follows:

- Phase velocity has a great effect on Kc_ℓ, λ_{max} and λ_N. With increasing phase velocity Kc_ℓ increases, and λ_{max} and λ_N decrease accordingly.
- The tube inclination also has an effect on Kc_ℓ, λ_{max} and λ_N. From downward flow to upward flow Kc_ℓ increases, and λ_{max} and λ_N decrease.
- Surface tension is a stable factor of the interface. With increasing surface tension, Kc_ℓ decreases, but λ_{max} and λ_N increase.

- The effect of liquid viscosity is very complicated and more further investigation is highly needed.

2. A set of non-linear hyperbolic governing equations was deduced from the complete two-fluid model equation by omitting the effect of the surface tension and assuming a quasi-steady-state for the gas phase. The propagation and growth of the interfacial disturbances were investigated by using the numerical method in terms of gas and liquid superficial velocities. The comparison of the results by non-linear stability analysis with those obtained from the linear stability analysis and experimental data was conducted. The non-linear stability analysis not only confirms the conclusions reached by the linear instability analysis, but also gives an insight into the growth and propagation of the interfacial disturbances on the interface of a gas–liquid two-phase flow.

Acknowledgements

This work is currently supported by the National Natural Science Foundation of China through contract No. 59995460-2 and National Science Foundation of China for Outstanding Young Scientist through contract No. 59725616.

References

[1] T.B. Banjamin, Shearing flow over a wavy boundary, J. Fluid Mech. 6 (1959) 161–205.
[2] J.W. Miles, On the generation of surface waves by shear flows, J. Fluid Mech. 3 (1957) 185–204.
[3] T.J. Hanratty, A. Hershman, Initiation of roll waves, AIChE J. 7 (1961) 488–497.
[4] T.J. Hanratty, J.M. Engen, Interaction between a turbulent air steam and a moving water surface, AIChE J. 3 (1957) 299–302.
[5] H. Jeffreys, On the formation of water waves by wind, Proc. R. Soc. A 107 (1925) 189.
[6] L.A. Jurman, M.J. Study of waves on thin liquid film sheared by turbulent gas flows, Phys. Fluids A 1 (1989) 522–536.
[7] N. Brauner, D.M. Maron, Stability analysis of stratified liquid–liquid flow, Int. J. Multiphase Flow 18 (1992) 103–121.
[8] D. Barnea, Y. Taitel, Kelvin–Helmholtz stability criteria for stratified flow, viscous versus non-viscous (invisid) approaches, Int. J. Multiphase Flow 19 (1993) 639–649.
[9] P.Y. Lin, T.J. Hanratty, Prediction of the initiation of slugs with linear stability theory, Int. J. Multiphase Flow 12 (1986) 79–98.
[10] D. Giovine, Stability of liquid flow down an inclined tube, Int. J. Multiphase Flow 17 (1991) 485–496.
[11] Y. Taitel, A.E. Dukler, A model for predicting flow regime transitions in horizontal and near horizontal gas–liquid flow, AIChE J. 22 (1976) 47–55.
[12] J.E. Kowalski, Wall and interfacial shear stress in stratified flow in a horizontal pipe, AIChE J. 33 (1987) 274–281.
[13] D. Barnea, Y. Taitel, Interfacial and structural stability of separated flow, Int. Multiphase Flow 20 (Suppl.) (1994) 387–414.
[14] X.M. Li, B. Ren, J.Q. Song, Parallel Algorithm and Numerical Solution of Partial Differential Equation, The University of Science and Technology for Defence Publishing Press, Changsha, China, 1990.
[15] J.M. Wang, Y. Sheng, Parallel Algorithm, National Defence Industry Publishing Press, Beijing, China, 1992.
[16] G.J. Li, Investigation on the characteristics of interfacial waves in gas–liquid two-phase flow through channels, Dissertation for Ph.D degree, Xi'an Jiaotong University, Xi'an, China, 1996.
[17] J. Shi, G. Kocamustafaogullari, Interfacial measurement in horizontal stratified flow patterns, Nucl. Eng. Des. 149 (1–3) (1994) 81–96.
[18] N. Andrtsos, T.J. Hanratty, Interfacial instabilities for horizontal gas–liquid flows in pipelines, Int. J. Multiphase Flow 13 (5) (1987) 583–603.
[19] C.J. Crowley, G.B. Wallis, J.J. Barry, Validation of a one-dimensional wave model for the stratified to slug flow regime transition, with consequences for wave growth and slug frequency, Int. J. Multiphase Flow 18 (2) (1992) 249–271.